Optics Letters

Time-reversed electromagnetic fields in anisotropic media

Elias Le Boudec,[1,*] Nicolas Mora,[2] Farhad Rachidi,[1] Marcos Rubinstein,[3] and Felix Vega[4]

[1]Ecole polytechnique fédérale de Lausanne, 1015 Lausanne, Vaud, Switzerland
[2]Universidad Nacional de Colombia, 111321 Bogotà D.C., Colombia
[3]University of Applied Sciences and Arts Western Switzerland, 1401 Yverdon-les-Bains, Vaud, Switzerland
[4]Technology Innovation Institute, Yas Island, Abu Dhabi, United Arab Emirates
*elias.leboudec@epfl.ch

Received 16 November 2023; revised 22 February 2024; accepted 27 February 2024; posted 28 February 2024; published 28 March 2024

Electromagnetic time reversal is commonly used for field imaging and focusing. This Letter builds upon the concept of the time-reversal cavity, which constitutes the main theoretical framework of time reversal theory. We study the behavior of the fields using modern methods of mathematical physics involving Colombeau generalized functions. This approach allows for a direct expression of time-reversed electric and magnetic fields in anisotropic time-reversal-invariant and nonreciprocal media. Moreover, the results hold for any arbitrary localized source and can readily be applied beyond the dipole approximation. Finally, a general result allows the prediction of the quality of focusing of the time-reversed fields as a function of the electrical permittivity and the magnetic permeability tensors in homogeneous anisotropic media, which contributes to the understanding of time reversal in complex media such as super-resolution enabling metamaterials.

https://doi.org/10.1364/OL.510604

In their Letter [1], Carminati *et al.* present an analytical procedure to derive the electric field obtained in a time-reversal cavity in electric anisotropic inhomogeneous media. In this setting, it is supposed that during the so-called direct-time phase, a localized source (in the case of [1], an infinitesimal electric dipole antenna) in an inhomogeneous volume V radiates electromagnetic fields. These fields are then recorded on the boundary ∂V of the volume, time-reversed, and emitted during the time-reversal phase. Note that the direct-time source is removed during the time-reversal phase. As in acoustics [2], we observe that the time-reversed fields converge to the direct-time source location while suffering from the diffraction limit. Because of this limitation, the fields are dispersed around the source location on a focal spot whose size is proportional to the medium wavelength. To overcome this limit, experimental solutions involving so-called "super-resolution" techniques enabled by local scatterers or metamaterials have been proposed in electromagnetism and acoustics [3,4]. While there has been a strong emphasis on medium inhomogeneity, the analysis of electromagnetic time reversal in anisotropic media is still missing and must be considered. The recent increase in the use of anisotropic metamaterials highlights the need for this analysis [5].

With this in mind, this Letter investigates the behavior of electromagnetic fields in the time-reversal cavity. It builds upon the theoretical framework proposed in [6] by analyzing the "microscopic" characteristics of the source, thanks to the use of Colombeau generalized functions, which also rely on Schwartz distributions [7–9]. These distributions offer the formal setting for dealing with partial differential equations such as Maxwell's equations, while Colombeau generalized functions allow distributions to be multiplied and undergo nonlinear transforms. Thanks to this formalism, the fundamental results of electric field time reversal presented in [1,6] can directly be applied to the magnetic and electric fields. Also, thanks to the broad scope of the reasoning, it is valid for arbitrary localized sources, including high-order multipole moments (e.g., quadrupole or octopoles) or non-singular current distributions (e.g., a current loop with finite cross-section). Furthermore, the derivation does not rely on the divergence theorem and can thus be applied to time-reversal-invariant nonreciprocal media as in [10]. Because of the link between time-reversal invariance, energy conservation, and reciprocity [11], such media must necessarily incorporate gains and losses. Finally, in homogeneous media, the results can be transformed to the wavenumber space, thanks to the Fourier transform of tempered Colombeau functions, allowing for a prediction of the focal spot size in general anisotropic media. We verify the results in a uniaxial dielectric anisotropic homogeneous medium, thanks to the knowledge of the analytical Green's function of this medium.

It must be noted that Colombeau generalized functions are not necessary in homogeneous media since solutions of Maxwell's equations can be treated with the convolution operator. The same holds for any linear partial differential equation with constant coefficients [12]. In inhomogeneous media, however, the solutions involve products of distributions in the most general settings, justifying the usage of Colombeau generalized

functions. Moreover, their use avoids the explicit need for regularization techniques for integrals containing poles [13] since this regularization is directly embedded in the structure of generalized functions.

First, we focus on the general derivation of the time-reversed fields. We work in frequency domain at a fixed ω, keep the ω dependence implicit, and make the following assumptions:

(1) The components of the magnetic field $\mathbf{B}$, the electric field $\mathbf{E}$, Green's functions, the current density $\mathbf{J}$, the location-dependent permittivity tensor ε, and the location-dependent permeability tensor μ belong to the set of tempered Colombeau generalized functions on $\mathbf{R}^3$, denoted by $\mathcal{G}_\tau(\mathbf{R}^3)$.

(2) Green's (generalized) functions G_e for the electric field and G_m for the magnetic field satisfy the usual wave equations:

$$\nabla \times \left(\mu^{-1}(\mathbf{r})\nabla \times (G_e(\mathbf{r},\mathbf{r}'))\right) - \omega^2 \varepsilon(\mathbf{r}) G_e(\mathbf{r},\mathbf{r}') = \delta(\mathbf{r}-\mathbf{r}')I \tag{1}$$

$$\nabla \times \left(\varepsilon^{-1}(\mathbf{r})\nabla \times \left(\mu^{-1}(\mathbf{r})G_m(\mathbf{r},\mathbf{r}')\right)\right) - \omega^2 G_m(\mathbf{r},\mathbf{r}') = \delta(\mathbf{r}-\mathbf{r}')I, \tag{2}$$

where $\nabla\times$ is the curl operator and $\mathbf{r}$ and $\mathbf{r}'$ are the spatial coordinates. Here, the equality is meant in $\mathcal{G}_\tau(\mathbf{R}^3)$, I is the 3×3 identity matrix, and $\delta \in \mathcal{G}_\tau(\mathbf{R}^3)$ satisfies

$$\iiint_{\mathbf{R}^3} \delta(\mathbf{r})\phi(\mathbf{r})\,\mathrm{d}^3\mathbf{r} = \phi(\mathbf{0}) \tag{3}$$

for all $\phi \in \mathcal{D}(\mathbf{R}^3)$, where $\mathcal{D}(\mathbf{R}^3)$ is the set of test functions on $\mathbf{R}^3$ (smooth functions with compact support). In other words, δ is a Colombeau generalized function such that its "distributional shadow" [8] is the usual Dirac δ distribution. More precisely, by considering all functions to be Colombeau generalized functions, we have introduced a degree of freedom corresponding to microscopic information. Equation (3) states that δ behaves macroscopically as the usual Dirac δ distribution. For simplicity, we will denote Eqs. (2) and (1) by

$$\mathcal{L}_e(\mathbf{r})G_e(\mathbf{r},\mathbf{r}') = \delta(\mathbf{r}-\mathbf{r}')I \tag{4}$$

$$\mathcal{L}_m(\mathbf{r})G_m(\mathbf{r},\mathbf{r}') = \delta(\mathbf{r}-\mathbf{r}')I, \tag{5}$$

where $\mathcal{L}_{m,e}(\mathbf{r})$ are the appropriate differential operators.

(3) The medium is time-reversal symmetric, but not necessarily reciprocal [10]. Hence, μ and ε (thus $\mathcal{L}_{m,e}$) are real, but might be asymmetric.

(4) We choose $G_{e,m}$ to be causal, i.e., the time-domain representation of $G_{e,m}$ has a support in $(-T,\infty)$ for some $T>0$.

(5) The electromagnetic fields $\mathbf{E},\mathbf{B}$ must satisfy the wave equations macroscopically:

$$\mathcal{L}_e(\mathbf{r})\mathbf{E}(\mathbf{r}) \asymp -j\omega\mathbf{J}(\mathbf{r}) \tag{6}$$

$$\mathcal{L}_m(\mathbf{r})\mathbf{B}(\mathbf{r}) \asymp \nabla \times \left(\varepsilon^{-1}(\mathbf{r})\mathbf{J}(\mathbf{r})\right) \triangleq \mathbf{J}_m(\mathbf{r}), \tag{7}$$

where $\asymp$ denotes the association between Colombeau generalized functions (i.e., the left- and right-hand sides of Eqs. (6) and (7) agree macroscopically), and $\triangleq$ indicates a definition.

Without loss of generality, let us focus on the magnetic field. As expected from the distribution theory (seeing Green's function as a particular fundamental solution of the differential equation, which also satisfies the boundary or radiation condition), a candidate for the magnetic field in direct time is given by

$$\mathbf{B}(\mathbf{r}) = \iiint_{\mathbf{R}^3} G_m(\mathbf{r},\mathbf{r}')\mathbf{J}_m(\mathbf{r})\,\mathrm{d}^3\mathbf{r}', \tag{8}$$

where the integrand is the product of the matrix G_m and the vector $\mathbf{J}_m(\mathbf{r})$ for fixed $\mathbf{r}$ and $\mathbf{r}'$. Indeed, let us fix $0<\beta<1$ and a Colombeau mollifier η and denote by $f^{(\beta,\eta)}$ a (smooth) representative of $f \in \mathcal{G}_\tau(\mathbf{R}^3)$. Then

$$\mathcal{L}_m^{(\beta,\eta)}(\mathbf{r})\mathbf{B}^{(\beta,\eta)}(\mathbf{r}) = \iiint_{\mathbf{R}^3} \mathcal{L}_m^{(\beta,\eta)}(\mathbf{r})G_m^{(\beta,\eta)}(\mathbf{r},\mathbf{r}')\mathbf{J}_m^{(\beta,\eta)}(\mathbf{r})\,\mathrm{d}^3\mathbf{r}', \tag{9}$$

since the integrand is smooth. By definition of Green's function G_m, the right-hand side is

$$\iiint_{\mathbf{R}^3} \delta^{(\beta,\eta)}(\mathbf{r}-\mathbf{r}')\mathbf{J}_m^{(\beta,\eta)}(\mathbf{r})\,\mathrm{d}^3\mathbf{r}', \tag{10}$$

which is associated with the right-hand side of Eq. (7) by Theorem 5.1.4 from [7]. Closely related to the direct-time solution $\mathbf{B}$, let us introduce the field $\widetilde{\mathbf{B}}$, defined as the causal field radiated by the time-reversed source. By linearity of the integral, this field $\widetilde{\mathbf{B}}$ is given by (here, * represents the complex conjugate)

$$\widetilde{\mathbf{B}}(\mathbf{r}) = \iiint_{\mathbf{R}^3} G_m(\mathbf{r},\mathbf{r}')\mathbf{J}_m^*(\mathbf{r})\,\mathrm{d}^3\mathbf{r}'. \tag{11}$$

Indeed,

$$\mathcal{L}_m(\mathbf{r})\widetilde{\mathbf{B}}(\mathbf{r}) \asymp \mathbf{J}_m^*(\mathbf{r}). \tag{12}$$

Next, notice that the time-reversed field $\mathbf{B}^*$ satisfies

$$\mathcal{L}_m^*(\mathbf{r})\mathbf{B}^*(\mathbf{r}) = \mathcal{L}_m(\mathbf{r})\mathbf{B}^*(\mathbf{r}) \asymp \mathbf{J}_m^*(\mathbf{r}) \tag{13}$$

because the coefficients of $\mathcal{L}_m$ are real. Thus, the time-reversal process yields the field

$$\mathbf{B}_{\mathrm{TRC}}(\mathbf{r}) = \mathbf{B}^*(\mathbf{r}) - \widetilde{\mathbf{B}}(\mathbf{r}) \tag{14}$$

$$= \iiint_{\mathbf{R}^3} \left[G_m^*(\mathbf{r},\mathbf{r}') - G_m(\mathbf{r},\mathbf{r}')\right]\mathbf{J}_m^*(\mathbf{r})\,\mathrm{d}^3\mathbf{r}'. \tag{15}$$

Indeed, by design, $\mathbf{B}_{\mathrm{TRC}}$ satisfies the homogeneous wave equation:

$$\mathcal{L}_m(\mathbf{r})\mathbf{B}_{\mathrm{TRC}}(\mathbf{r}) \asymp 0. \tag{16}$$

This is necessary since no source is present during the time-reversal phase. Moreover, by the causality of Green's function, $\mathbf{B}_{\mathrm{TRC}}$ corresponds to the time-reversed field $\mathbf{B}^*$ at (sufficiently) negative times. Afterward, $\mathbf{B}^*$ mixes with the causal diverging (or outgoing) wave $\widetilde{\mathbf{B}}$, yielding the usual diffraction limit. In the same manner, we obtain

$$\mathbf{E}_{\mathrm{TRC}}(\mathbf{r}) \asymp -j\omega \iiint_{\mathbf{R}^3} \left[G_e^*(\mathbf{r},\mathbf{r}') - G_e(\mathbf{r},\mathbf{r}')\right]\mathbf{J}^*(\mathbf{r})\,\mathrm{d}^3\mathbf{r}'. \tag{17}$$

The time-reversal formulas given in Eqs. (14) and (17) are valid for any localized source. Indeed, modeling the source $\mathbf{J}$ as a tempered Colombeau generalized function is a weak hypothesis. In particular, the results hold for any tempered distribution. For example, electrically large sources modeled as multipole moments require high-order derivatives of the Dirac δ distribution. By definition, these result in spatial derivatives of Green's function. As a complement to [1], notice that if $\mathbf{J}$ corresponds to a dipole source, the magnetic field amplitude is minimal at the origin. By Eq. (15), the time-reversed field also exhibits

this property. Finally, the presented approach is valid for time-reversal-invariant nonreciprocal media, as the operators $\mathcal{L}_{m,e}$ need only to be real, not symmetric, which is necessary in [1] because of the divergence theorem.

Now that we have highlighted the link between Green's functions and the time-reversed electromagnetic fields, we focus on the quality of focusing (i.e., the reciprocal of the diffraction spot size) of the time-reversed fields in homogeneous anisotropic media. First, we perform a Fourier transform of the spatial variables and express Eq. (1) as a function of the wavenumber $\mathbf{k} = \begin{bmatrix} k_x & k_y & k_z \end{bmatrix}$:

$$K(\mathbf{k})\mu^{-1}K(\mathbf{k})G_e(\mathbf{k}) + \omega^2\varepsilon G_e(\mathbf{k}) \asymp I, \tag{18}$$

where the matrix $K(\mathbf{k})$ represents the curl operator [14]. It is clear that Green's function is determined by the inverse of the matrix:

$$A(\mathbf{k}) \triangleq K(\mathbf{k})\mu^{-1}K(\mathbf{k}) + \omega^2\varepsilon, \tag{19}$$

which can be symbolically written as [15]

$$A^{-1}(\mathbf{k}) = \frac{\mathrm{adj}(A(\mathbf{k}))}{\det(A(\mathbf{k}))}, \tag{20}$$

where $\mathrm{adj}(A(\mathbf{k}))$ is the adjugate matrix of A. Similar to [16], we introduce the set $\mathcal{S} = \left\{\mathbf{k} \in \mathbf{R}^3 : \det(A(\mathbf{k})) = 0\right\}$ that describes the dispersion relation at a given frequency ω. In isotropic media, $\mathcal{S}$ is a sphere of radius $k_0 = \omega/c$ centered at the origin, where c is the speed of light in the medium. A possible solution of the homogeneous equation

$$A(\mathbf{k})G_h(\mathbf{k}) \asymp 0 \tag{21}$$

is given by

$$G_h(\mathbf{k}) = \mathrm{adj}(A(\mathbf{k}))g_h(\mathbf{k}), \quad g_h(\mathbf{k}) = \alpha(\mathbf{k})\delta_{\mathcal{S}}(\mathbf{k}), \tag{22}$$

where $\alpha, \delta_{\mathcal{S}}$ are tempered Colombeau generalized functions and $\delta_{\mathcal{S}}$ has a distributional shadow that corresponds to the Dirac δ distribution on the surface $\mathcal{S}$. Indeed, we have

$$A(\mathbf{k})G_h(\mathbf{k}) = A(\mathbf{k})\mathrm{adj}(A(\mathbf{k}))g_h(\mathbf{k}) = \det(A(\mathbf{k}))\alpha(\mathbf{k})\delta_{\mathcal{S}}(\mathbf{k}). \tag{23}$$

By the argument presented in [16], this corresponds to Eq. (21) since on the support of $\delta_{\mathcal{S}}$, $\det(A(\mathbf{k}))$ is zero. Next, we must determine the direction dependence $\alpha(\mathbf{k})$. Equation (15) imposes G_h to be the spatial Fourier transform of a purely imaginary function. Since μ and ε are real, this translates to the parity condition:

$$\alpha(-\mathbf{k}) = -\alpha(\mathbf{k})^*. \tag{24}$$

In isotropic media, the rotation invariance of the radiating condition sets [16] $\alpha(\mathbf{k}) = C \in \mathbb{C}$. It is sufficient for C to be purely imaginary for the parity condition in Eq. (24) to hold. In turn, the focusing pattern is given by the inverse Fourier transform:

$$g_h(\mathbf{r}) = \frac{C}{(2\pi)^3}\int_{\mathcal{S}} e^{j\mathbf{k}\cdot\mathbf{r}}\,\mathrm{d}^2S. \tag{25}$$

It is straightforward to verify that, as expected, g_h is given by a sinc function in isotropic media.

In anisotropic media, we propose, as a heuristic, to work with the same constant-$\alpha(\mathbf{k})$ ansatz. While it is necessary to verify that a proper choice of C satisfies a radiation condition of the corresponding Green's function, this verification goes beyond the scope of this article as many anisotropic Green's functions are yet to be discovered. Moreover, the rotational variance in anisotropic media is captured by the dispersion relation even for a constant $\alpha(\mathbf{k})$. Furthermore, we will see that this simple ansatz allows to predict the focusing pattern. Finally, note that the choice of a constant $\alpha(\mathbf{k})$ corresponds to the radiation of a Dirac δ distribution. Allowing $\alpha(\mathbf{k})$ to vary may embed higher-order multipole moments, describing the radiation of intricate and electrically large current distributions.

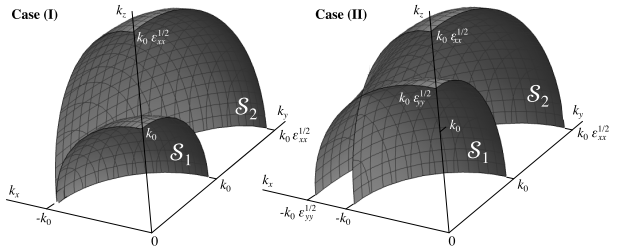

Fig. 1. One octant of the dispersion relations for case (I) (uniaxial medium with $\varepsilon_{xx} = 4$) and case (II) (biaxial medium with $\varepsilon_{xx} = 4$, $\varepsilon_{yy} = 2$). We denote the inner surface by $\mathcal{S}_1$ and the outer surface by $\mathcal{S}_2$.

This derivation is valid for any anisotropic homogeneous media. We turn our attention to two cases:

(I) Uniaxial dielectric anisotropic homogeneous media, characterized by a scalar magnetic permeability and a permittivity tensor given by $\varepsilon = \varepsilon_0\varepsilon_r\mathrm{Diag}(\varepsilon_{xx}, 1, 1)$ for some $\varepsilon_{xx}>0$.
(II) Biaxial dielectric anisotropic homogeneous media, characterized by a scalar magnetic permeability and a permittivity tensor given by $\varepsilon = \varepsilon_0\varepsilon_r\mathrm{Diag}(\varepsilon_{xx}, \varepsilon_{yy}, 1)$ for some $\varepsilon_{xx}, \varepsilon_{yy}>0$.

Figure 1 presents the dispersion relations for the two cases. They are formed by two surfaces $\mathcal{S}_1$ and $\mathcal{S}_2$. We call the solution corresponding to a single surface a mode. Next, we perform a numerical integration of Eq. (25) separately on each mode to obtain g_h, plotted in Fig. 2. Finally, [17] provides the analytical form of Green's function for uniaxial media (case I). Figure 3 then presents the diffraction pattern resulting from the time reversal, given by $G_e(\mathbf{r}) - G_e^*(\mathbf{r})$. The two modes are visible in Green's function. Indeed, the focus is homogeneous on the x and y axes, with a wavelength corresponding to vacuum. This corresponds to $\mathcal{S}_1$ on the xy axes. On the other hand, the wavelength shortens along the z axis, a feature of $\mathcal{S}_2$. What is more, this shortening corresponds to a factor $\sqrt{\varepsilon_{xx}}$, which is visible in the dispersion relation or $g_h(x, y, 0)$ in Fig. 2. A similar argument can be made for the other axis pairs. Also, the transverse dimensions of the dispersion relations translate directly into the wavelength of the corresponding inverse Fourier transforms. The first mode in the uniaxial medium is isotropic, while it is anisotropic in the biaxial medium. This anisotropy is influenced by ε_{yy} only, and the wavelength in the z axis is reduced by a factor $\sqrt{\varepsilon_{yy}}$. A similar reasoning applies to the second mode.

It is worth mentioning that the anisotropic Green's function in Fig. 3 can be explained by two phenomena only: on the one hand, the well-known dipole radiation in isotropic, homogeneous media, and on the other hand, a direction-dependent scaling of the coordinates. This scaling can be predicted by the inverse Fourier transform of the dispersion relation g_h. The latter is thus central to understanding the effect of medium anisotropy on the convergence of time reversal. A straightforward integration can predict the shape of the focus and, therefore, its

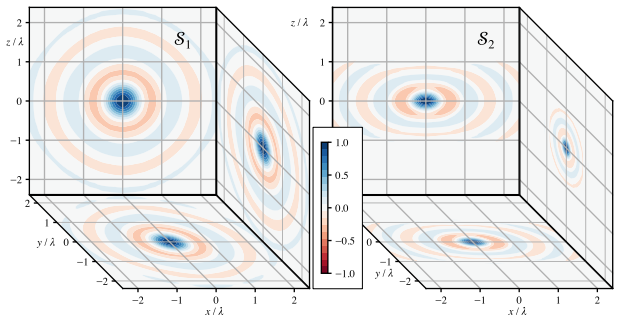

(a) Case (I), uniaxial medium with $\varepsilon_{xx} = 4$.

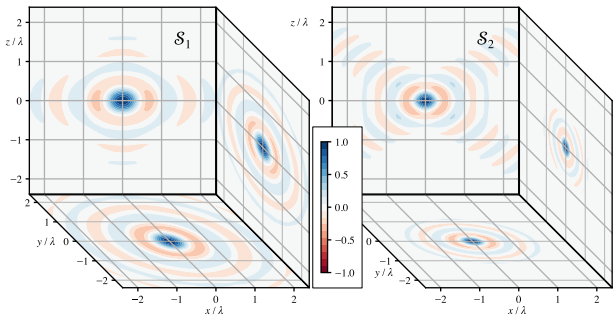

(b) Case (II), biaxial medium with $\varepsilon_{xx} = 4$, $\varepsilon_{yy} = 2$.

Fig. 2. Plane cuts of the focusing pattern $g_h(\mathbf{r})$ obtained by numerical integration of the dispersion relations in Fig. 1. For clarity, the pattern is decomposed into two functions, each obtained by integrating over the surfaces $\mathcal{S}_1$ and $\mathcal{S}_2$. The color bar indicates the normalized amplitude.

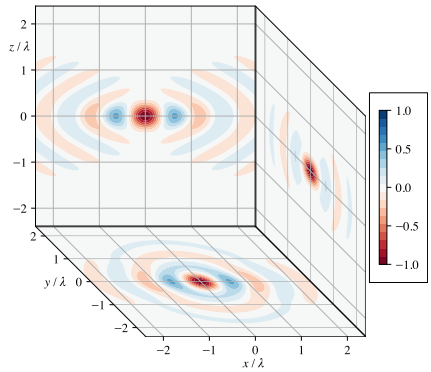

Fig. 3. Plane cuts of the time-reversed field $G_e(\mathbf{r}) - G_e^*(\mathbf{r})$ obtained from Green's function of the uniaxial medium (case (I)). We show only the components of Green's function matrix at index (3, 3), corresponding to the z-component of the radiation of an electric dipole polarized along the z-axis. The color bar indicates the amplitude, normalized to the highest value among all three plots. Light gray corresponds to zero.

quality—based solely on the dispersion relation. This quantity is available for arbitrary homogeneous media, for which Green's function is usually unavailable directly. For example, for biaxial media, Fig. 2 predicts an improvement in focusing dependent on the square roots of the eigenvalues of the permittivity tensor. Also, this improvement depends both on the axis the field is looked at and the chosen field component.

Thanks to the proposed approach, it is possible to assess the performance of the time-reversal process in anisotropic media. In particular, the approach predicts the resolution limit imposed by the superposition of the converging and diverging wavefronts for sources beyond the dipole approximation. This prediction matters for practical imaging or focusing experiments combined with resolution-enhancing metamaterials. Indeed, the analysis of such metamaterials may rely on anisotropic effective constitutive parameters. Examples include hyperbolic wire media based on silicon pillar arrays [18] or control over the dispersion through a dielectric coating [19]. While the effective medium might not be appropriate for resonant systems [20], dielectric metalenses are still desirable for loss mitigation. In these cases, the proposed analysis enables the design of subwavelength imaging systems. Finally, the technique opens the door to wave focusing or imaging in nonreciprocal media.

Funding. Technology Innovation Institute (TII/DERC/2254/2021).

Acknowledgment. We thank H. Karami, A. Mostajabi, Z. Wang, S. Tkachenko, N. Dietler, and J.-Y. Le Boudec for their helpful comments.

Disclosures. The authors declare no conflicts of interest.

Data availability. No data were generated or analyzed in the presented research.

REFERENCES

1. R. Carminati, R. Pierrat, J. D. Rosny, *et al.*, Opt. Lett. **32**, 3107 (2007).
2. M. Fink, IEEE Trans. Ultrason., Ferroelect., Freq. Contr. **39**, 555 (1992).
3. F. Lemoult, G. Lerosey, J. de Rosny, *et al.*, Phys. Rev. Lett. **104**, 203901 (2010).
4. B. Orazbayev and R. Fleury, Phys. Rev. X **10**, 031029 (2020).
5. X. Zhang and Y. Wu, Sci. Rep. **5**, 7892 (2015).
6. J. de Rosny, G. Lerosey, and M. Fink, IEEE Trans. Antennas Propag. **58**, 3139 (2010).
7. J. F. Colombeau, *Elementary Introduction to New Generalized Functions* (Elsevier, 1985).
8. A. Gsponer, Eur. J. Phys. **30**, 109 (2008).
9. G. van Dijk, *Distribution Theory: Convolution, Fourier Transform, and Laplace Transform* (De Gruyter, 2013).
10. S. Buddhiraju, A. Song, G. T. Papadakis, *et al.*, Phys. Rev. Lett. **124**, 257403 (2020).
11. H. A. Haus, *Waves and Fields in Optoelectronics* (Prentice-Hall, 1984).
12. D. Mitrea, *Distributions, Partial Differential Equations, and Harmonic Analysis* (Springer-Verlag, 2013).
13. A. Gsponer, Eur. J. Phys. **28**, 267 (2007).
14. J. R. Wait, J. Res. Natl. Bur. Stand., Sect. B **68B**, 119 (1964).
15. J. A. Bennett, J. Plasma Phys. **15**, 133 (1976).
16. J. A. Schmalz, G. Schmalz, T. E. Gureyev, *et al.*, Am. J. Phys. **78**, 181 (2010).
17. T. G. Mackay and A. Lakhtakia, *Electromagnetic Anisotropy and Bianisotropy – A Field Guide*, 2nd ed. (World Scientific, 2019).
18. A. Kannegulla and L.-J. Cheng, Opt. Lett. **41**, 3539 (2016).
19. J. S. Brownless, B. C. P. Sturmberg, A. Argyros, *et al.*, J. Opt. Soc. Am. B **34**, 472 (2017).
20. A. B. Kozyrev, C. Qin, I. V. Shadrivov, *et al.*, Opt. Express **15**, 11714 (2007).